ACS OMEGA

http://pubs.acs.org/journal/acsodf

Article

Computational Insights into the Regeneration of Ovothiol and Ergothioneine and Their Selenium Analogues by Glutathione

Jesse B. Elder, Joshua A. Broome, and Eric A. C. Bushnell*

Cite This: *ACS Omega* 2022, 7, 31813−31821

Read Online

ACCESS | Metrics & More | Article Recommendations | Supporting Information

ABSTRACT: Ovothiol and ergothioneine are powerful antioxidants that readily react with oxidants by forming their respective disulfides. In fact, ovothiol is widely considered one of the most powerful natural antioxidants. However, for these antioxidants to be again involved in reacting with oxidants, they must be regenerated via the reduction of the disulfide bonds. In the present work, the regeneration of the antioxidants ovothiol and ergothioneine and their selenium analogues, by the closed-shell nucleophilic attack of glutathione, was investigated using density functional theory. From the calculated thermodynamic data, the attack of glutathione on OSSO and EYYE (where Y = S and/or Se) will readily occur in solution. Moreover, in comparison to the reference reaction GSH + GSSG → GSSG + GSH, all reactions are expected to be faster. Overall, the results presented herein show that the key antioxidant GSH should readily recycle ovothiol, ovoselenol, ergothioneine, and ergoseloneine from OYYO and EYYE (where Y = S and/or Se).

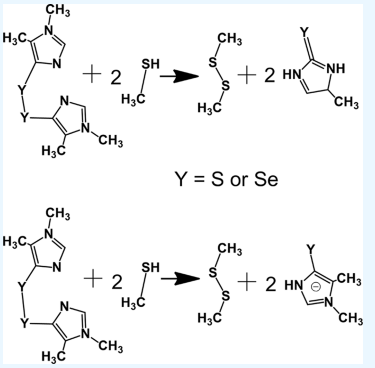

INTRODUCTION

Reactive oxygen species (ROSs) have important roles within our bodies. Under normal physiological conditions, ROSs are constantly being produced during metabolic processes.[1] ROSs are also produced pathologically in many ways, for example, from exposure to ionizing radiation and the presence of free-metal ions.[2−4] It is when the concentration of ROSs become too high that negative effects on DNA, proteins, and lipids occur, resulting in oxidative stress that leads to mutations, misfolding of proteins, and possibly cell death.[5−10] Notably, oxidative stress has been shown to be linked to many diseases such as cancer, Alzheimer's disease, Parkinson's disease, and type-2 diabetes.[6,11−15]

To combat the harmful effects of ROSs, cells use antioxidants to mitigate, repair, or prevent oxidative damage. Antioxidants may directly interact with ROSs or the molecules that produce ROSs, such as free-metal ions, thus preventing the creation of ROSs.[16−19] One of the major antioxidants in the human body is glutathione (Scheme 1a), a cysteine-based tripeptide, with a reactive thiol group. To prevent oxidative damage by ROSs, glutathione, undergoes a one-electron oxidation, resulting in a short-lived sulfur radical species that readily joins with another glutathione radical species to form a stable disulfide. The disulfide form of glutathione is then readily acted upon by glutathione reductase via a nucleophilic disulfide exchange reaction to regenerate an active glutathione molecule.[20] In addition to reacting with ROSs, glutathione is known to assist in the regeneration of other antioxidants, such as vitamin E.[21] Although glutathione is one of the most ubiquitous antioxidants, there are many other antioxidants that

Scheme 1. An Illustration of (a) Glutathione, (b) Ovothiol (Ovothiol$_A$, n = 0; Ovothiol$_B$, n = 1; and Ovothiol$_C$, n = 2), and (c) Ergothioneine, in Their Dominant Form at Biological pH

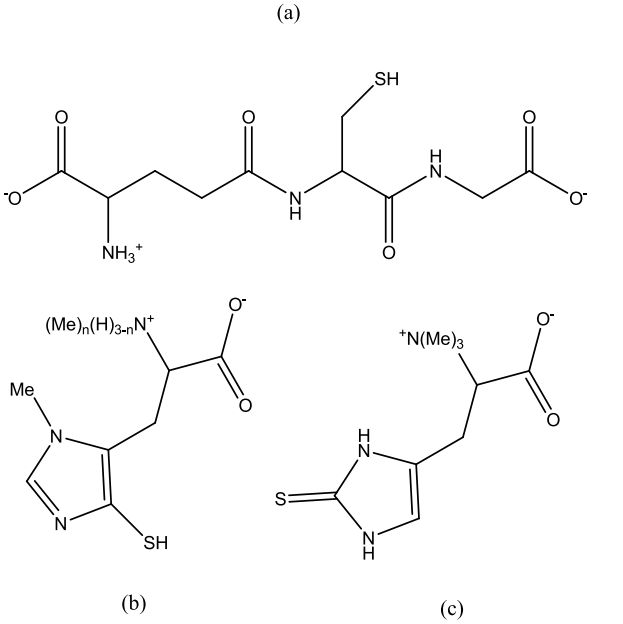

Received: April 21, 2022
Accepted: July 18, 2022
Published: August 31, 2022

exist in nature. Two such antioxidants are the mercaptohistidine derivatives, ovothiol and ergothioneine.

Ovothiol is widely considered one of the most powerful natural antioxidants, and it exists in three naturally occurring forms depending on the degree of methylation of the alpha-amino nitrogen (Scheme 1b).[22] However, as discussed by de Luna et al.,[23] past experimental work has shown that the deletion of the amino acid portion of ovothiol had little effect on its chemistry and therefore the oxidative power of ovothiol is a result of the mercaptohistidine functional group.[24,25] While ovothiol is not naturally synthesized in humans, it can be taken in through our diet. Given its antioxidant strength, ovothiol and its analogues have been gaining increasing attention as potential therapeutics for use in humans. Indeed, $Ovothiol_A$ has been reported to induce autophagy in liver carcinoma cell lines, suggesting a potential role in regulating cancer cell growth.[26,27]

First discovered in ergot fungus, ergothioneine (Scheme 1c), like ovothiol, is not naturally produced in humans but is taken up through our diets. An important source of ergothioneine is mushrooms, where it is proposed to have an anti-oxidative and anti-inflammatory role.[28,29] In humans, the exact role of ergothioneine is unknown, although in animal trials, it has been found in high concentrations in tissues and cells that experience high oxidative stress, such as the liver, erythrocytes, eye cornea, and kidneys.[30−34] It is noted that aerosols containing ergothioneine have been developed to treat chronic inflammatory diseases such as asthma.[25,35,36] At biological pH, ergothioneine predominantly exists in its thione tautomer form, making ergothioneine very stable and resistant to auto-oxidation and a slight resistance to form disulfide.[37] Like ovothiol, past experimental work has shown that the deletion of the amino acid portion of ergothioneine has little effect on its chemistry.[24,25]

Sulfur appears in group 16 of the periodic table, along with the other chalcogens. Selenium lies directly below sulfur on the periodic table, resulting in sulfur and selenium sharing similar chemical and physical properties.[38,39] Like sulfur, selenium has the ability to act as an antioxidant, though a mechanism by which selenium prevents oxidative damage can vary from that of sulfur since selenium's reductive ability is stronger than that of sulfur.[40−42] However, while the two elements share many similarities, there are some important differences.[43] For instance, thiol/disulfide exchange reactions are accelerated in solution with the replacement of S by Se because of selenolate being both a better nucleophile and a better leaving group than thiolate.[44,45] In fact, it has been stated that almost all chemical reactions involving Se are faster than the analogous reactions involving sulfur.[43] In previous studies,[23,46] the ability of ovothiol, ergothioneine, ovoselenol, and ergoseloneine to prevent the (Cu^{II}/Cu^{I}) redox cycling in solution was investigated. It is noted that Cu^{I} ions catalyze the Fenton-type reaction with H_2O_2, resulting in the formation of a hydroxide and hydroxyl radical. The results of these past studies found that, in the case of ovothiol and ergothioneine and their selenium analogues, the reduction of Cu^{II} to Cu^{I} with the concomitant formation of the disulfide or diselenide was thermodynamically favorable.[23,46] It was concluded that ovothiol, ergothioneine, ovoselenol, and ergoseloneine are able to prevent (Cu^{II}/Cu^{I}) redox cycling and are therefore suitable for the protection of copper-induced oxidative damage.[23,46] However, with the formation of the disulfide and diselenides, it is unclear if the reduced forms of these powerful antioxidants would be regenerated in vivo.

Previous experimental and theoretical work has investigated the dichalcogenide exchange reaction for the nucleophilic attack of a thiolate or selenite on a di-chalcogen bond, in both the gas phase and condensed phase.[45,47−51] However, the past theoretical work used small models, consisting of a methyl or hydrogen as a side chain on the chalcogen.[49] Thus, it is unclear how the presence of the imidazole rings of ovothiol, ergothioneine, and their selenium analogues will have an effect on the kinetics and thermodynamics of the substitution reactions. Herein, the thermodynamics and kinetics of the nucleophilic attack of glutathione to regenerate ovothiol, ergothioneine, and their selenium analogues was investigated using density functional theory (DFT). To the best of our knowledge, this work represents the first investigation of the regeneration of the antioxidants ovothiol and ESH or their selenium analogues by glutathione.

METHODS

As discussed above, because past experimental work[24,25] has shown the deletion of the amino acid portion of ovothiol and ergothioneine has little effect on their chemistry, the molecules ovothiol, ergothioneine, ovoselenol, and ergoseloneine have been modeled as 4-thiol-N1-methyl-5-methylimidazole, 4-selenol-N1-methyl-5-methylimidazole, 2-thione-4-methylimidazole, and 2-selone-4-methylimidazole, respectively, to reduce computational costs. For simplicity, they will be referred to as OSH, OSeH, ESH, and ESeH, respectively. In the case of glutathione, to reduce computational costs it has been modeled as methane thiol and will henceforth be referred to as GSH. The disulfide, diselenide, and mixed sulfide selenide molecules will be referred to as OYYO and EYYE, where Y = S or Se. The chemical reactions investigated herein are given in Table 1.

Table 1. Dichalcogenide Exchange Reactions Investigated in the Present Work[a]

	reaction	Y_1	Y_2
1	GSH + GSSG → GSSG + GSH	N/A	N/A
2	GSH + OSSO → GSSO + OSH	S	S
3	GSH + OSSeO → GSSO + OSeH	S	Se
4	GSH + OSeSO → GSSeO + OSH	Se	S
5	GSH + OSeSeO → GSSeO + OSeH	Se	Se
6	GSH + ESSE → GSSE + ESH	S	S
7	GSH + ESSeE → GSSE + ESeH	S	Se
8	GSH + ESeSE → GSSeE + ESH	Se	S
9	GSH + ESeSeE → GSSeE + ESeH	Se	Se
10	GSH + GSSO → GSSG + OSH	S	N/A
11	GSH + GSSeO → GSSG + OSeH	Se	N/A
12	GSH + GSSE → GSSG + ESH	S	N/A
13	GSH + GSSeE → GSSG + ESeH	Se	N/A

[a]The Gibbs reaction energies ($\Delta_r G°$) and Gibbs activation energies ($\Delta_r G^{‡}$), obtained at the SMD-M06-2X/aug-cc-pVTZ//SMD-M06-2X/aug-Cc-pVDZ level of theory, for these reactions are shown in Figures 1−5. The labels Y_1 and Y_2 are used in Figures 1−5.

All calculations were done using the Gaussian 09 and Gaussian 16 software suites.[52,53] Optimized geometries and harmonic vibrational frequencies were obtained at the SMD-M06-2X/aug-cc-pVDZ level of theory, where water was chosen as the solvent.[54−58] The use of SMD continuum method has been shown to be a valid approach to optimize structures in

https://doi.org/10.1021/acsomega.2c02506
ACS Omega 2022, 7, 31813−31821

the condensed phase.[59] All calculations were done using the keyword integral = grid = ultrafine. For all disulfide exchange reactions, the transition states (TSs), a relaxed scan approach, was used where the $GS^{-}\cdots YEYE$, $GS^{-}\cdots YOYO$, $GS^{-}\cdots SMeYE$, and $GS^{-}\cdots SMeOE$ distances were initially set to 3.8 Å. As the nucleophilic GS^{-} approached the electrophilic Y, if a maximum in energy was observed in the PES, the structure at this maximum in PE was used as a starting guess for a TS. The standard Berny algorithm was used to optimize the TS. The nature of the TS was visually confirmed via the visualization of a single imaginary frequency using GaussView 5.[60] The optimized geometries of all complexes are provided in the Supporting Information (Table S1). IRC calculations in the forward and reverse direction were done at the SMD-M06-2X/aug-cc-pVDZ level of theory to confirm nature of the TSs. For the IRC calculations, 20 steps were followed in both the forward and reverse directions. Following the 20 steps in the forward and reverse directions, the SMD-M06-2X/aug-cc-pVDZ level of theory was then used to fully optimize the reactant and product complexes. The *xyz* coordinates of the reactant and product complexes are provided in Table S2. Notably, the IRC calculations confirm that the TSs obtained using the standard Berny algorithm are the TSs for the disulfide exchange reactions discussed herein.

As noted in the Introduction, previous work has investigated the reaction mechanisms that involve S or Se acting as the nucleophile, electrophile, and/or leaving group, where the moiety attached to the chalcogen atom was a hydrogen atom or methyl group.[49] From the work, it was found that, in solution, the substitution reaction can occur via two mechanisms. The first mechanism is a one-step reaction (i.e., SN_2-type mechanism), whereas the other mechanism is a two-step process.[49] Regarding the SN_2-type mechanism, a single TS exists for the disulfide exchange reaction. The second mechanism, referred to as an addition−elimination mechanism, involves the formation of a hypervalent intermediate (i.e., a sulfur with more than four electron groups surrounding it). However, from the past work, it was concluded that, in solution, the SN_2 mechanism is more likely.[49] It is noted that in the present investigation, attempts to find a stable hypervalent sulfur/selenium intermediate failed at the SMD-M06-2X/aug-cc-pVDZ level of theory. Thus, for the disulfide exchange reactions involving OYYO and EYYE, only a single TS, corresponding to the backside attack of the electrophile by the nucleophile, characteristic of a classic SN_2 type reaction, was found. Regarding the SN_2-type TS, it can proceed via a *syn*- or *anti*-conformation of the nucleophile and the leaving group.[49] However, past evidence has shown little difference in the energy of the *syn*- or *anti*-TS for the reaction mechanisms regardless of whether sulfur or selenium is acting as the nucleophile, electrophile, and/or leaving group.[49] Given that the past work only looked at systems where the moiety attached to the sulfur/selenium was a methyl group or hydrogen atom, it is expected that the larger and bulkier side group on the electrophile and leaving group would result in the *syn*-conformers to experience enhanced steric repulsion. Thus, for the reactions discussed herein, the *anti*-TSs of all disulfides, diselenides, and mixed sulfide−selenides were solely investigated.

Single point energies were obtained at the SMD-M06-2X/aug-cc-pVTZ//SMD-M06-2X/aug-cc-pVDZ level of theory.[58] Gibbs reaction and activation energies were determined by correcting the single point energies by adding the Gibbs energy correction ($\Delta_r G^{\circ}_{corr}$) obtained from the harmonic frequency calculations. Per the work by Galano and Alvarez-Idaboy,[61] the $\Delta_r G_s^{\circ}$ values were corrected to a standard state of 1 M. The solvent cage effects on the enthalpy and entropy of activation have been included according to the corrections proposed by Okuno that consider the free volume theory.[62,63]

Implicit solvation models do not properly treat hydrogen bonding interactions between solvent and solutes. In aqueous solution, this can result in large errors in the calculated values such as pK_as.[64] A number of studies have shown that inclusion of explicit waters to account for hydrogen bonding between solute and solvent improves the calculation of pK_as, especially for processes involving ionic species, which are generally prone to more error.[64−74] A previous study demonstrated that for thiols the inclusion of explicit waters near the sulfur was essential for obtaining reasonable pK_as when using implicit solvation models to treat effects of the bulk solvent on the solute.[64] Specifically, it was found that when three explicit water molecules were included to hydrogen bond to the acidic sulfur, good agreement between calculated and experimental pK_a values was achieved.[64] It was concluded that regarding SMD, the lack of short-range hydrogen bonding interactions is a major factor in the poor performance for calculating thiol pK_as.[64] A past study showed that when calculating the pK_as of thiols, the wB97XD DFT functional in combination with a basis set includes polarization functions on the hydrogens and diffuse functions on the heavy atoms is required.[64] Thus to calculate all Gibbs deprotonation energies, the wB97XD/aug-cc-pVDZ level of theory was used for geometry optimizations, calculation of Gibbs corrections and electronic energies. The Gibbs reaction energies for the deprotonation of GSH, OSH, ESH, OSeH, and ESeH were calculated, where the standard chemical potential of a proton in a dilute aqueous environment ($\mu^0_{298K}(H^+)$) was chosen to be −1130.5 kJ mol^{-1} at a pH of zero.[64]

RESULTS AND DISCUSSION

As done in previous work[64] we have included three explicit water molecules that forms hydrogen bonds with both the thiol and the thiolate of methane thiol/thiolate. The water molecules were arranged such that the total number of hydrogen bonds were the same for the thiol and the thiolate. This was done to ensure that the calculated energy difference is a result of the change in the strength of hydrogen bonds and not from the change in the number of hydrogen bonds.[64] Given that the thione tautomer form of ESH is favored over the thiol form, it is the imidazole ring involved in gaining and losing a proton. Thus, in the case of ESH and OSH due to the imidazole ring, an additional water molecule was included to a total of four water molecules.

The commonly accepted pK_a for methanethiol is 10.4, whereas for ovothiol, a pK_a of 6.7 was used for the SH group.[75] For ESH, a value of 11.2 was used for the deprotonation of the imidazole nitrogen.[76] These values correspond to Gibbs deprotonation energies at the standard pH of 60.0, 38.2, and 78.6 kJ mol^{-1}. As seen in Table 2 the calculated Gibbs deprotonation energy for GSH is in excellent agreement with experiment with an unsigned error of only 0.6 kJ mol^{-1}. For OSH and ESH the calculated values are on an average only 9.0 kJ mol^{-1} more endergonic and are therefore in reasonable agreement with experiment. It is noted that in the absence of any explicit water molecules, the calculated Gibbs deprotonation energies for GSH, OSH, and ESH are on an average 36.8

https://doi.org/10.1021/acsomega.2c02506
ACS Omega 2022, 7, 31813−31821

Table 2. Gibbs Reaction Energies ($\Delta_rG°$) at pH = 0 for the Deprotonation of GSH, OSH, OSeH, ESH, and ESeH Obtained at the SMD-M06-2X/aug-cc-pVTZ//SMD-M06-2X/aug-cc-pVDZ Level of Theory[a]

reaction	calculated $\Delta_rG°$	experimental $\Delta_rG°$
$GSH \rightarrow GS^- + H^+$	60.0	59.4[b]
$OSH \rightarrow OS^- + H^+$	49.3	38.2[c]
$OSeH \rightarrow OSe^- + H^+$	32.0	N/A
$ESH \rightarrow ES^- + H^+$	70.8	64.0[d]
$ESeH \rightarrow ESe^- + H^+$	76.4	N/A

[a]All energies are in kJ Mol^{-1}. For the calculation of the Gibbs deprotonation energies $\mu^0_{298K}(H^+)$ was chosen to be −1130.5 kJ Mol^{-1} (see Computational Methods).[64] [b]$\Delta_rG°$ for deprotonation of GSH was determined from the commonly accepted experimental pK_a value of 10.4 for methanethiol. [c]$\Delta_rG°$ for deprotonation of OSH was calculated from experimental pK_a value of 6.7.[75] [d]$\Delta_rG°$ for deprotonation of ESH was determined from experimental pK_a value 11.2.[76]

kJ mol^{-1}, more endergonic than the experimental Gibbs deprotonation energies. Thus, given the reasonable agreement between calculated and experimental Gibbs energies for deportation of GSH, OSH, and ESH, and given the fact that experimental Gibbs deprotonation energies for the OSeH and ESeH are unavailable we have decided to use the calculated energies in Table 2 for the Gibbs energy surfaces shown in Figures 12345.

Thermodynamics and Kinetics for the Attack of GSH to OYYO and EYYE. To better understand the effect of the imidazole ring on the thermodynamics and kinetics of the substitution reaction, the Gibbs activation energy ($\Delta_rG^‡$) for the reference reaction GSH + GSSG → GSSG + GSH was calculated (Figure 1). For the reference reaction $\Delta_rG^‡$ was calculated to be 115.3 kJ mol^{-1} under standard conditions. Notably, the value of $\Delta_rG^‡$ as shown in Figure 1 is the largest Gibbs activation energy and is therefore predicted to be the slowest disulfide exchange reaction investigated herein. Given that the reactants and products are the same in Reaction 1, $\Delta_rG° = 0.0$ kJ mol^{-1}.

As seen in Figures 2 and 3 the dichalcogenide exchange reactions involving OSSO and ESSE are predicted to occur with a value of $\Delta_rG^‡$ less than that seen for the reference Reaction 1 (Table 1). Regarding the disulfide OSSO, the value of $\Delta_rG^‡$ for the substitution (i.e., Reaction 2) is approximately 10.5 kJ mol^{-1} lower in energy than that for Reaction 1. For ESSE (i.e., Reaction 6), $\Delta_rG^‡$ is 37.5 kJ mol^{-1} lower in energy than the value for Reaction 1. Thus, it is expected that in solution the rate at which GSH attacks OSSO and ESSE would be greater than that seen for the attack of GSSG.

For OSSeO, the substitution of the S in the Leaving Group (LG) with Se (i.e., Reaction 3) accelerates the substitution further, where $\Delta_rG^‡$ is 15.8 kJ mol^{-1} lower in energy than that for Reaction 1. Similarly, for ESSeE, the substitution of the S in the LG with Se (Reaction 7) further accelerates the dichalcogenide exchange reaction, where $\Delta_rG^‡$ was calculated to be 44.6 kJ mol^{-1} lower than that for Reaction 1. As noted above for Reactions 4, 5, 8, and 9, a classic SN_2-type TS could not be found at the present level of theory. However, considering the reduction in $\Delta_rG^‡$ for Reactions 2, 3, 6, and 7 relative to Reaction 1 (Table 1), the presence of the imidazole ring results in the acceleration of the dichalcogenide exchange reaction. Additionally, comparing Figures 2 and 3, the reactions involving EYYE have Gibbs activation energies that are considerably less than the Gibbs activation energies for the reactions involving OYYO. A partial explanation for the difference in activation energies may be a result of ES^- (and subsequently ESH) predominantly existing in its thione tautomer form where cleavage of the dichalcogenide bond results in the negative change of EY^- being delocalized into the imidazole ring rather than being localized on the chalcogen atom like that seen for OS^-.

For the optimized TSs (Table S1), the average distance between the electrophilic chalcogen atoms and nucleophilic CH_3S^- was calculated to be 2.84 Å, with a standard deviation of 0.09 Å. The average angle of attack of the nucleophile was calculated to be 172.0°, with a standard deviation of 0.9°. The average dihedral angle between the leaving group and nucleophile (Figure S1) was found to be 127.5°, with a standard deviation of 17.6°. It is noted that because of the hydrogen bond seen in the EYYE system the dihedral angle is approximately 35° smaller than that seen for the OYYO systems. With an average dihedral angle of 127.5° it is apparent that the TSs for dichalcogenide exchange reaction exists in an *anti*-conformation. Overall, the substitution of the sulfur by a selenium has a marginal effect on the structure of the classic SN_2 type TS regardless of choice of chalcogen atom.

From the thermodynamic data provided in Figure 2, it can be seen that with protonation of OS^- and OSe^- the attack of

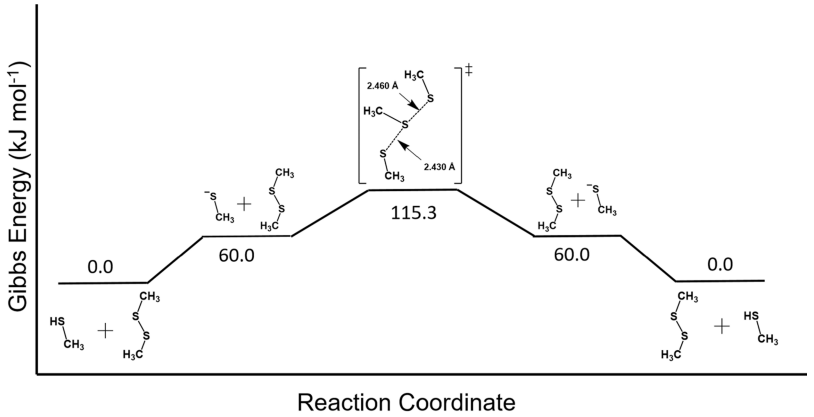

Figure 1. Gibbs energy surface for Reaction 1 (Table 1). Energies obtained at the SMD-M06-2X/aug-cc-pVTZ//SMD-M06-2X/aug-cc-pVDZ level of theory. For the deprotonation in the first step and protonation in the last step the Gibbs energies from Table 2 were used.

https://doi.org/10.1021/acsomega.2c02506
ACS Omega 2022, 7, 31813−31821

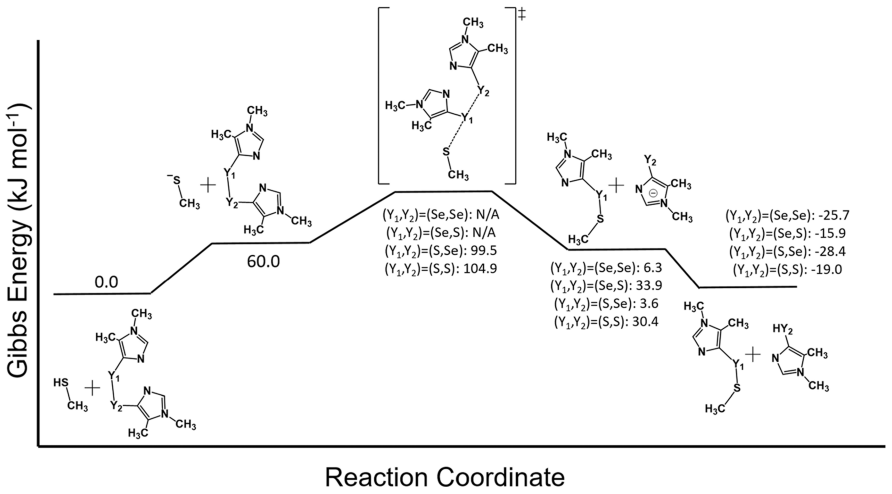

Figure 2. Gibbs energy surface for the attack of CH_3SH to OY_1Y_2O to form CH_3SY_1O + OY_2H (Table 1, Reactions 2−5) at pH = 0. Energies obtained at the SMD-M06-2X/aug-cc-pVTZ//SMD-M06-2X/aug-cc-pVDZ level of theory. For the deprotonation in the first step and protonation in the last step the Gibbs energies from Table 2 were used.

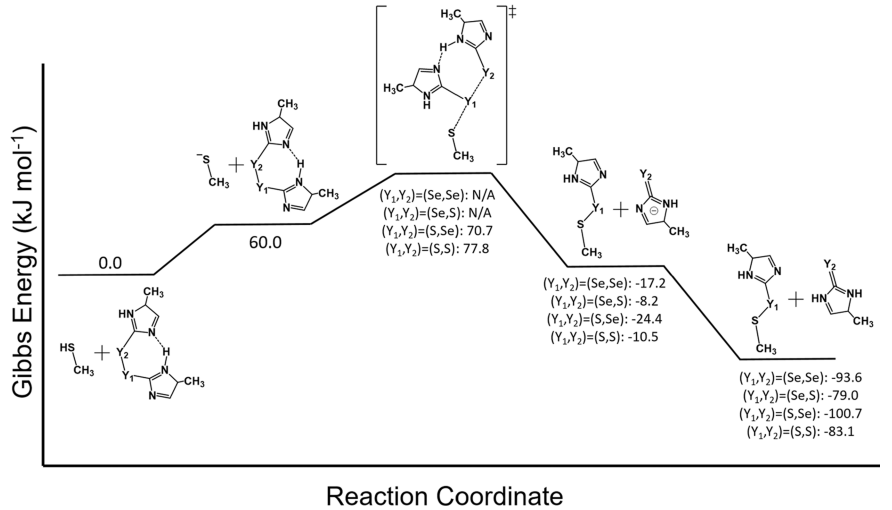

Figure 3. Gibbs energy surface for the attack of CH_3SH to EY_1Y_2E to form CH_3SY_1E + EY_2H (Table 1, Reactions 6−9) at pH = 0. Energies obtained at the SMD-M06-2X/aug-cc-pVTZ//SMD-M06-2X/aug-cc-pVDZ level of theory. For the deprotonation in the first step and protonation in the last step the Gibbs energies from Table 2 were used.

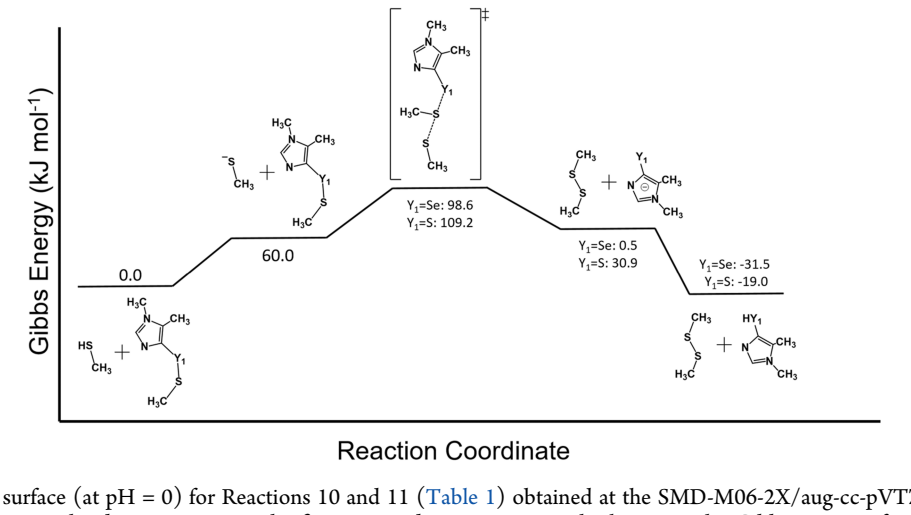

Figure 4. Gibbs energy surface (at pH = 0) for Reactions 10 and 11 (Table 1) obtained at the SMD-M06-2X/aug-cc-pVTZ//SMD-M06-2X/aug-cc-pVDZ level of theory. For the deprotonation in the first step and protonation in the last step, the Gibbs energies from Table 2 were used.

https://doi.org/10.1021/acsomega.2c02506
ACS Omega 2022, 7, 31813−31821

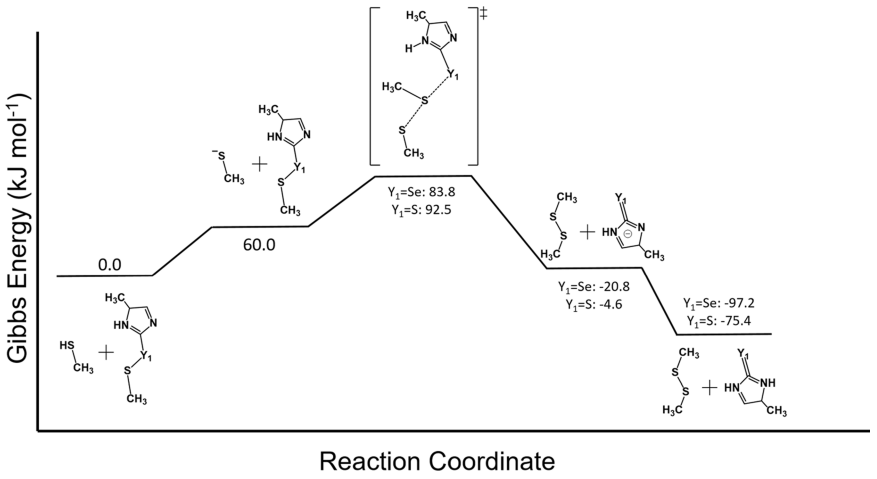

Figure 5. Gibbs energy surface (at pH = 0) for Reactions 12 and 13 (Table 1) obtained at the SMD-M06-2X/aug-cc-pVTZ//SMD-M06-2X/aug-cc-pVDZ level of theory. For the deprotonation in the first step and protonation in the last step, the Gibbs energies from Table 2 were used.

GSH on OYYO is exergonic. However, the reaction is most exergonic when Y_2 = Se (i.e., Reactions 3 and 5). From Figure 3, the reactions where GSH attacks EYYE are all considerably exergonic at the present level of theory. Overall, the reactions involving EYYE are generally 66.3 kJ mol^{-1} more exergonic than the analogous OYYO reactions.

Thermodynamics and Kinetics for the Attack of GSH to GSYO and GSYE. With the formation of GSYO and GSYE, the attack of GSH to form GSSG, OYH, and EYH (Table 1, Reactions 10−13) was investigated. For the optimized TSs in Figures 4 and 5, the average distance between the electrophile and nucleophile was calculated to be 2.750 Å, with a standard deviation of 0.090 Å. The average angle of attack of the nucleophile was calculated to be 175.0°, with a standard deviation of 0.8°. The average dihedral angle between the leaving group and nucleophile (Figure S1) was found to be 123.8°, with a standard deviation of 18.5°.

The Gibbs energy surfaces for Reactions 10−13 are shown in Figures 4 and 5. As seen in Figures 4 and 5, the attack of GSH to GSYO and GSYE occurs with Gibbs activation energies ($\Delta_r G^{\ddagger}$) less than that for Reaction 1. Therefore, at the present level of theory it is expected that the attack of GSH to GSYO and GSYE would occur quicker than that for GSSG. These results are in agreement with the past experimental work that has shown that OSH acts in tandem with glutathione, where OSH neutralizes oxidants forming OSSO with GSH then used to maintain ovothiol in the reduced state.[77] Moreover, previous experimental work has shown that glutathione reductase can reduce ESSE, but only with the aid of glutathione.[78] However, looking at Figures 2 and 5, the second disulfide exchange reaction is generally slower than the respective first disulfide exchange reaction. Specifically, comparing Reactions 10 and 2, Reactions 10 and 3, Reactions 12 and 6, and Reactions 12 and 7, the Gibbs activation energies of the second step are on average 8.2 kJ mol^{-1} more endergonic. From previous experimental work,[77] it was found that at a pH of 7.2, Gibbs activation energies of 73.0 and 80.9 kJ mol^{-1} are calculated for GSH + OSSO and GSH + GSSO, respectively. In correcting the values to a pH of 7.2 as in Figures 2 and 4 for reactions GSH + OSSO and GSH + GSSO, the Gibbs activation energies were calculated to be 64.7 and 68.9 kJ mol^{-1}, respectively. Thus, agreement between theory and experiment is good. Moreover, in agreement with the experiment, the second step (i.e., attack of GSH + GSSO) is slower than the first step (i.e., attack of GSH + OSSO).[77]

Regarding the thermodynamic values in Figure 4, it can be seen that only the dichalcogenide exchange reaction between GSH and GSYO is thermodynamically likely to occur when Y_1 = S. In the case where Y1 = Se, the overall change in Gibbs energy is +19.8 kJ mol^{-1}. However, the reactions involving GSYE are considerably exergonic. Looking at Figure 5, the process of dichalcogenide exchange is most thermodynamically favorable when Y1 = Se and occurs with $\Delta_r G^{\circ}$ = −45.2 kJ mol^{-1}. When Y1 = S, the value of $\Delta_r G^{\circ}$ is −44.8 kJ mol^{-1}. As noted above, the greater exergonicity for the reaction between GSH and GSYE is likely a result of ESH predominantly existing in its thione tautomer form. Given the exergonicity of the reactions involving EYYE, GSH, therefore, has the thermodynamic driving force to attack EYYE to regenerate EYH.

As noted in the Introduction, previous work has shown that for OSH, ESH, OSeH, and ESeH, the reduction of Cu(II) to Cu(I) with concomitant formation of the disulfide is thermodynamically favorable.[23,46] Importantly, the results presented herein show that the key antioxidant GSH can readily attack OYYO and EYYE (where Y = S and/or Se), resulting in regeneration of the powerful respective antioxidants with Gibbs activation energy less than that for the disulfide exchange reaction between GSH and GSSG. However, from the results presented in Figures 1−5, the dichalcogenide exchange reaction is exergonic under standard conditions for the reaction of GSH with OSSO or EYYE to form the respective products GSSG + 2OSH and GSSG + 2EYH. Therefore, the ability to regenerate OSH and EYH under standard conditions offers a means to mitigate Cu-induced oxidative damage via the formation of the respective OSSO and EYYE. Moreover, given that the human body naturally produces GSH, the formed OSSO and EYYE is reacted upon by GSH to reform the powerful OSH and EYH antioxidants and GSSG. The importance of it is that, in the human body, GSSG is readily acted upon by glutathione reductase to regenerate the active GSH molecule, whereas OSH and EYH are not naturally produced in humans.

https://doi.org/10.1021/acsomega.2c02506
ACS Omega 2022, 7, 31813−31821

CONCLUSIONS

Past work has shown that the reduction of Cu(II) to Cu(I) with concomitant formation of the disulfide (OYYO and EYYE (where Y = S and/or Se)) is thermodynamically feasible for OYH, and EYH.[23,46] In the present work, DFT was used to study the regeneration of the antioxidants OYH and EYH (where Y = S or Se), via the nucleophilic attack of GSH on OYYO and EYYE. Importantly at the SMD-M06-2X/aug-cc-pVTZ//SMD-M06-2X/aug-cc-pVDZ level of theory, the key antioxidant GSH will readily attack OSSO and EYYE (where Y = S and/or Se), resulting in the regeneration of the powerful antioxidants OSH and EYH, respectively in an overall exergonic reaction. Thus, the calculated Gibbs activation energies suggest that the attack of glutathione on OSSO and EYYE (where Y = S and/or Se) will readily occur in solution.

ASSOCIATED CONTENT

Supporting Information

The Supporting Information is available free of charge at https://pubs.acs.org/doi/10.1021/acsomega.2c02506.

The dihedral angle (θ) between the leaving group and nucleophile. (a) shows the labeling and (b) shows the dihedral angle (θ) as shown in Figure S1. The *xyz* coordinates of the complexes discussed in the present article are provided in Table S1 (PDF)

AUTHOR INFORMATION

Corresponding Author

Eric A. C. Bushnell − *Department of Chemistry, Brandon University, Brandon, Manitoba R7A 6A9, Canada;* orcid.org/0000-0002-2252-9920; Email: bushnelle@brandonu.ca

Authors

Jesse B. Elder − *Department of Chemistry, Brandon University, Brandon, Manitoba R7A 6A9, Canada*

Joshua A. Broome − *Department of Chemistry, Brandon University, Brandon, Manitoba R7A 6A9, Canada*

Complete contact information is available at: https://pubs.acs.org/10.1021/acsomega.2c02506

Funding

E.A.C.B. thanks the Natural Sciences and Engineering Research Council of Canada (NSERC) for funding. J.B.E. thanks NSERC and BU for an NSERC USRA.

Notes

The authors declare no competing financial interest.

E.A.C.B., J.B.E., and J.A.B. thank WESTGRID, SHARCNET and Compute Canada for computational resources.

REFERENCES

(1) Finkel, T. Signal transduction by reactive oxygen species. *J. Cell Biol.* **2011**, *194*, 7−15.

(2) Di Meo, S.; Reed, T. T.; Venditti, P.; Victor, V. M. Role of ROS and RNS Sources in Physiological and Pathological Conditions. *Oxid. Med. Cell. Longevity* **2016**, *44*, No. 1245049.

(3) Persson, H. L.; Kurz, T.; Eaton, J. W.; Brunk, U. T. Radiation-induced cell death: importance of lysosomal destabilization. *Biochem. J.* **2005**, *389*, 877−884.

(4) Halliwell, B.; Gutteridge, J. M. C. Role of Free-Radicals and Catalytic Metal-Ions in Human-Disease - An Overview. *Methods Enzymol.* **1990**, *186*, 1−85.

(5) Beckman, K. B.; Ames, B. N. Oxidative decay of DNA. *J. Biol. Chem.* **1997**, *272*, 19633−19636.

(6) Behl, C.; Moosmann, B. Oxidative nerve cell death in Alzheimer's disease and stroke: Antioxidants as neuroprotective compounds. *Biol. Chem.* **2002**, *383*, 521−536.

(7) Berlett, B. S.; Stadtman, E. R. Protein oxidation in aging, disease, and oxidative stress. *J. Biol. Chem.* **1997**, *272*, 20313−20316.

(8) Gutteridge, J. M. C. Lipid-Peroxidation and Antioxidants as Biomarkers of Tissue-Damage. *Clin. Chem.* **1995**, *41*, 1819−1828.

(9) Sies, H. Oxidative stress: Oxidants and antioxidants. *Exp. Physiol.* **1997**, *82*, 291−295.

(10) Hausladen, A.; Stamler, J. S. Nitrosative stress. *Methods Enzymol.* **1999**, *300*, 389−395.

(11) Zekry, D.; Epperson, T. K.; Krause, K. H. A role for NOX NADPH oxidases in Alzheimer's disease and other types of dementia? *IUBMB Life* **2003**, *55*, 307−313.

(12) Waris, G.; Ahsan, H. Reactive oxygen species: role in the development of cancer and various chronic conditions. *J. Carcinog.* **2006**, *5*, 14.

(13) Zhang, Y.; Dawson, V. L.; Dawson, T. M. Oxidative stress and genetics in the pathogenesis of Parkinson's disease. *Neurobiol. Dis.* **2000**, *7*, 240−250.

(14) Hernandez-Mijares, A.; Rocha, M.; Apostolova, N.; Borras, C.; Jover, A.; Banuls, C.; Sola, E.; Victor, V. M. Mitochondrial complex I impairment in leukocytes from type 2 diabetic patients. *Free Radical Biol. Med.* **2011**, *50*, 1215−1221.

(15) Evans, J. L.; Goldfine, I. D.; Maddux, B. A.; Grodsky, G. M. Oxidative stress and stress-activated signaling pathways: A unifying hypothesis of type 2 diabetes. *Endocr. Rev.* **2002**, *23*, 599−622.

(16) Hanlon, D. P. Interaction of Ergothioneine with Metal Ions and Metalloenzymes. *J. Med. Chem.* **1971**, *14*, 1084.

(17) Motohashi, N.; Mori, I.; Sugiura, Y.; Tanaka, H. Metal-Complexes of Ergothioneine. *Chem. Pharm. Bull.* **1974**, *22*, 654−657.

(18) Bailly, F.; Azaroual, N.; Bernier, J. L. Design, synthesis and glutathione peroxidase-like properties of ovothiol-derived diselenides. *Bioorg. Med. Chem.* **2003**, *11*, 4623−4630.

(19) Miyoshi, N.; Takabayashi, S.; Osawa, T.; Nakamura, Y. Benzyl isothiocyanate inhibits excessive superoxide generation in inflammatory leukocytes: implication for prevention against inflammation-related carcinogenesis. *Carcinogenesis* **2004**, *25*, 567−575.

(20) Couto, N.; Malys, N.; Gaskell, S. J.; Barber, J. Partition and Turnover of Glutathione Reductase from Saccharomyces cerevisiae: A Proteomic Approach. *J. Proteome Res.* **2013**, *12*, 2885−2894.

(21) Niki, E.; Tsuchiya, J.; Tanimura, R.; Kamiya, Y. Regeneration of Vitamin-E from Alpha-Chromanoxyl Radical by Glutathione and Vitamin-C. *Chem. Lett.* **1982**, *6*, 789−792.

(22) Marjanovic, B.; Simic, M. G.; Jovanovic, S. V. Heterocyclic Thiols as Antioxidants - Why Ovothiol-C is a Better Antioxidant Than Ergothioneine. *Free Radical Biol. Med.* **1995**, *18*, 679−685.

(23) De Luna, P.; Bushnell, E. A. C.; Gauld, J. W. A Density Functional Theory Investigation into the Binding of the Antioxidants Ergothioneine and Ovothiol to Copper. *J. Phys. Chem. A* **2013**, *117*, 4057−4065.

(24) Asmus, K. D.; Bensasson, R. V.; Bernier, J. L.; Houssin, R.; Land, E. J. One-electron oxidation of ergothioneine and analogues investigated by pulse radiolysis: Redox reaction involving ergothioneine and vitamin C. *Biochem. J.* **1996**, *315*, 625−629.

(25) Hand, C. E.; Taylor, N. J.; Honek, J. F. Ab initio studies of the properties of intracellular thiols ergothioneine and ovothiol. *Bioorg. Med. Chem. Lett.* **2005**, *15*, 1357−1360.

(26) Castellano, I.; Migliaccio, O.; D'Aniello, S.; Merlino, A.; Napolitano, A.; Palumbo, A. Shedding light on ovothiol biosynthesis in marine metazoans. *Sci. Rep.* **2016**, *6*, 11.

(27) Russo, G. L.; Russo, M.; Castellano, I.; Napolitano, A.; Palumbo, A. Ovothiol Isolated from Sea Urchin Oocytes Induces Autophagy in the Hep-G2 Cell Line. *Mar. Drugs* **2014**, *12*, 4069−4085.

(28) Barger, G.; Ewins, A. J. CCLVII—The constitution of ergothioneine: a betaine related to histidine. *J. Chem. Soc., Trans.* **1911**, *99*, 2336−2341.
(29) Ito, T.; Kato, M.; Tsuchida, H.; Harada, E.; Niwa, T.; Osawa, T. Ergothioneine as an Anti-Oxidative/Anti-Inflammatory Component in Several Edible Mushrooms. *Food Sci. Technol. Res.* **2011**, *17*, 103−110.
(30) Deiana, M.; Rosa, A.; Casu, V.; Piga, R.; Dessi, M. A.; Aruoma, O. I. L-Ergothioneine modulates oxidative damage in the kidney and liver of rats in vivo: studies upon the profile of polyunsaturated fatty acids. *Clin. Nutr.* **2004**, *23*, 183−193.
(31) Bedirli, A.; Sakrak, O.; Muhtaroglu, S.; Soyuer, I.; Guler, I.; Erdogan, A. R.; Sozuer, E. M. Ergothioneine pretreatment protects the liver from ischemia-reperfusion injury caused by increasing hepatic heat shock protein 70. *J Surg Res.* **2004**, *122*, 96−102.
(32) Kumosani, T. A. L-ergothioneine level in red blood cells of healthy human males in the Western province of Saudi Arabia. *Exp. Mol. Med.* **2001**, *33*, 20−22.
(33) Salt, H. B. The ergothioneine content of the blood in health and disease. *Biochem. J.* **1931**, *25*, 1712−1719.
(34) Shires, T. K.; Brummel, M. C.; Pulido, J. S.; Stegink, L. D. Ergothioneine distribution in bovine and porcine ocular tissues. *Comp. Biochem. Physiol., Part C: Pharmacol., Toxicol. Endocrinol.* **1997**, *117*, 117−120.
(35) Rahman, I.; Gilmour, P. S.; Jimenez, L. A.; Biswas, S. K.; Antonicelli, F.; Aruoma, O. I. Ergothioneine inhibits oxidative stress- and TNF-alpha-induced NF-kappa B activation and interleukin-8 release in alveolar epithelial cells. *Biochem. Biophys. Res. Commun.* **2003**, *302*, 860−864.
(36) Kirkham, P.; Rahman, I. Oxidative stress in asthma and COPD: Antioxidants as a therapeutic strategy. *Pharmacol. Ther.* **2006**, *111*, 476−494.
(37) Cheah, I. K.; Halliwell, B. Ergothioneine; antioxidant potential, physiological function and role in disease. *Biochim. Biophys. Acta, Mol. Basis Dis.* **2012**, *1822*, 784−793.
(38) Jacob, C.; Giles, G. L.; Giles, N. M.; Sies, H. Sulfur and selenium: The role of oxidation state in protein structure and function. *Angew. Chem., Int. Ed.* **2003**, *42*, 4742−4758.
(39) Ip, C.; Ganther, H. E. Comparison of selenium and sulfur analogs in cancer prevention. *Carcinogenesis* **1992**, *13*, 1167−1170.
(40) Battin, E. E.; Brumaghim, J. L. Antioxidant Activity of Sulfur and Selenium: A Review of Reactive Oxygen Species Scavenging, Glutathione Peroxidase, and Metal-Binding Antioxidant Mechanisms. *Cell Biochem. Biophys.* **2009**, *55*, 1−23.
(41) Pearson, J. K.; Boyd, R. J. Modeling the reduction of hydrogen peroxide by glutathione peroxidase mimics. *J. Phys. Chem. A* **2006**, *110*, 8979−8985.
(42) Pearson, J. K.; Boyd, R. J. Density functional theory study of the reaction mechanism and energetics of the reduction of hydrogen peroxide by ebselen, ebselen diselenide, and ebselen selenol. *J. Phys. Chem. A* **2007**, *111*, 3152−3160.
(43) Reich, H. J.; Hondal, R. J. Why Nature Chose Selenium. *ACS Chem. Biol.* **2016**, *11*, 821−841.
(44) O'Keefe, J. P.; Dustin, C. M.; Barber, D.; Snider, G. W.; Hondal, R. J. A "Seleno Effect" Differentiates the Roles of Redox Active Cysteine Residues in Plasmodium falciparum Thioredoxin Reductase. *Biochemistry* **2018**, *57*, 1767−1778.
(45) Pleasants, J. C.; Guo, W.; Rabenstein, D. L. A comparative study of the kinetics of selenol/diselenide and thiol/disulfide exchange reactions. *J. Am. Chem. Soc.* **1989**, *111*, 6553−6558.
(46) Wiebe, J.; Zaliskyy, V.; Bushnell, E. A. C. A Computational Investigation of the Binding of the Selenium Analogues of Ergothioneine and Ovothiol to Cu(I) and Cu(II) and the Effect of Binding on the Redox Potential of the Cu(II)/Cu(I) Redox Couple. *J. Chem.* **2019**, No. 9593467.
(47) Kice, J. L.; Slebockatilk, H. Reactivity of Nucleophiles toward and the Site of Nucleophilic-Attack on Bis(Alkylthio) Selenides. *J. Am. Chem. Soc.* **1982**, *104*, 7123−7130.
(48) Bachrach, S. M.; Mulhearn, D. C. Nucleophilic substitution at sulfur: S(N)2 or addition-elimination? *J. Phys. Chem.* **1996**, *100*, 3535−3540.
(49) Bachrach, S. M.; Demoin, D. W.; Luk, M.; Miller, J. V. Nucleophilic Attack at Selenium in Diselenides and Selenosulfides. A Computational Study. *J. Phys. Chem. A* **2004**, *108*, 4040−4046.
(50) Bachrach, S. M.; Woody, J. T.; Mulhearn, D. C. Effect of ring strain on the thiolate-disulfide exchange. A computational study. *J. Org. Chem.* **2002**, *67*, 8983−8990.
(51) Bachrach, S. M.; Chamberlin, A. C. Theoretical study of nucleophilic substitution at the disulfide bridge of cyclo-L-cystine. *J. Org. Chem.* **2003**, *68*, 4743−4747.
(52) Frisch, M. J.; Trucks, G. W.; Schlegel, H. B.; Scuseria, G. E.; Robb, M. A.; Cheeseman, J. R.; Scalmani, G.; Barone, V.; Mennucci, B.; Petersson, G. A.; Nakatsuji, H.; Caricato, M.; Li, X.; Hratchian, H. P.; Izmaylov, A. F.; Bloino, J.; Zheng, G.; Sonnenberg, J. L.; Hada, M.; Ehara, M.; Toyota, K.; Fukuda, R.; Hasegawa, J.; Ishida, M.; Nakajima, T.; Honda, Y.; Kitao, O.; Nakai, H.; Vreven, T.; Montgomery, J. A., Jr.; Peralta, J. E.; Ogliaro, F.; Bearpark, M. J.; Heyd, J. J.; Brothers, E. N.; Kudin, K. N.; Staroverov, V. N.; Kobayashi, R.; Normand, J.; Raghavachari, K.; Rendell, A. P.; Burant, J. C.; Iyengar, S. S.; Tomasi, J.; Cossi, M.; Rega, N.; Millam, J. M.; Klene, M.; Knox, J. E.; Cross, J. B.; Bakken, V.; Adamo, C.; Jaramillo, J.; Gomperts, R.; Stratmann, R. E.; Yazyev, O.; Austin, A. J.; Cammi, R.; Pomelli, C.; Ochterski, J. W.; Martin, R. L.; Morokuma, K.; Zakrzewski, V. G.; Voth, G. A.; Salvador, P.; Dannenberg, J. J.; Dapprich, S.; Daniels, A. D.; Farkas, Ö.; Foresman, J. B.; Ortiz, J. V.; Cioslowski, J.; Fox, D. J. *Gaussian 09 Rev. E.01*, Gaussian, Inc.: Wallingford, CT, 2009.
(53) Frisch, M. J.; Trucks, G. W.; Schlegel, H. B.; Scuseria, G. E.; Robb, M. A.; Cheeseman, J. R.; Scalmani, G.; Barone, V.; Petersson, G. A.; Nakatsuji, H.; Li, X.; Caricato, M.; Marenich, A. V.; Bloino, J.; Janesko, B. G.; Gomperts, R.; Mennucci, B.; Hratchian, H. P.; Ortiz, J. V.; Izmaylov, A. F.; Sonnenberg, J. L.; Williams; Ding, F.; Lipparini, F.; Egidi, F.; Goings, J.; Peng, B.; Petrone, A.; Henderson, T.; Ranasinghe, D.; Zakrzewski, V. G.; Gao, J.; Rega, N.; Zheng, G.; Liang, W.; Hada, M.; Ehara, M.; Toyota, K.; Fukuda, R.; Hasegawa, J.; Ishida, M.; Nakajima, T.; Honda, Y.; Kitao, O.; Nakai, H.; Vreven, T.; Throssell, K.; Montgomery, J. A., Jr.; Peralta, J. E.; Ogliaro, F.; Bearpark, M. J.; Heyd, J. J.; Brothers, E. N.; Kudin, K. N.; Staroverov, V. N.; Keith, T. A.; Kobayashi, R.; Normand, J.; Raghavachari, K.; Rendell, A. P.; Burant, J. C.; Iyengar, S. S.; Tomasi, J.; Cossi, M.; Millam, J. M.; Klene, M.; Adamo, C.; Cammi, R.; Ochterski, J. W.; Martin, R. L.; Morokuma, K.; Farkas, O.; Foresman, J. B.; Fox, D. J. *Gaussian 16 Rev. B.01*; Wallingford, CT, 2016.
(54) Marenich, A. V.; Cramer, C. J.; Truhlar, D. G. Universal Solvation Model Based on Solute Electron Density and on a Continuum Model of the Solvent Defined by the Bulk Dielectric Constant and Atomic Surface Tensions. *J. Phys. Chem. B* **2009**, *113*, 6378−6396.
(55) Mardirossian, N.; Head-Gordon, M. How Accurate Are the Minnesota Density Functionals for Noncovalent Interactions, Isomerization Energies, Thermochemistry, and Barrier Heights Involving Molecules Composed of Main-Group Elements? *J. Chem. Theory Comput.* **2016**, *12*, 4303−4325.
(56) Zhao, Y.; Truhlar, D. G. The M06 Suite Of Density Functionals For Main Group Thermochemistry, Thermochemical Kinetics, Noncovalent Interactions, Excited States, And Transition Elements: Two New Functionals And Systematic Testing Of Four M06-Class Functionals And 12 Other Functionals. *Theor. Chem. Acc.* **2008**, *120*, 215−241.
(57) Zhao, Y.; Truhlar, D. G. Density Functionals With Broad Applicability In Chemistry. *Acc. Chem. Res.* **2008**, *41*, 157−167.
(58) Pritchard, B. P.; Altarawy, D.; Didier, B.; Gibson, T. D.; Windus, T. L. New Basis Set Exchange: An Open, Up-to-Date Resource for the Molecular Sciences Community. *J. Chem. Inf. Model.* **2019**, *59*, 4814−4820.
(59) Ribeiro, R. F.; Marenich, A. V.; Cramer, C. J.; Truhlar, D. G. Use of Solution-Phase Vibrational Frequencies in Continuum Models

https://doi.org/10.1021/acsomega.2c02506
ACS Omega 2022, 7, 31813−31821

for the Free Energy of Solvation. *J. Phys. Chem. B* **2011**, *115*, 14556−14562.
(60) Frisch, M. J.; Hratchian, H. P.; Dennington, II, R. D.; Keith, T. A.; Millam, J.; Nielsen, A. B.; Holder, A. J.; Hiscocks, J. *GaussView 5*; Gaussian, Inc.: Wallingford, CT, 2009.
(61) Galano, A.; Alvarez-Idaboy, J. R. A computational methodology for accurate predictions of rate constants in solution: Application to the assessment of primary antioxidant activity. *J. Comput. Chem.* **2013**, *34*, 2430−2445.
(62) Okuno, Y. Theoretical investigation of the mechanism of the baeyer-villiger reaction in nonpolar solvents. *Chemistry* **1997**, *3*, 212−218.
(63) Benson, S. W. *The foundation of chemical kinetics*; McGraw-Hill: New-York, 1960.
(64) Thapa, B.; Schlegel, H. B. Density Functional Theory Calculation of pKa's of Thiols in Aqueous Solution Using Explicit Water Molecules and the Polarizable Continuum Model. *J. Phys. Chem. A* **2016**, *120*, 5726−5735.
(65) Pliego, J. R.; Riveros, J. M. Theoretical calculation of pK(a) using the cluster-continuum model. *J. Phys. Chem. A* **2002**, *106*, 7434−7439.
(66) Kelly, C. P.; Cramer, C. J.; Truhlar, D. G. Adding Explicit Solvent Molecules to Continuum Solvent Calculations for the Calculation of Aqueous Acid Dissociation Constants. *J. Phys. Chem. A* **2006**, *110*, 2493−2499.
(67) Adam, K. R. New Density Functional and Atoms in Molecules Method of Computing Relative pKa Values in Solution. *J. Phys. Chem. A* **2002**, *106*, 11963−11972.
(68) Bryantsev, V. S.; Diallo, M. S.; Goddard, W. A., III Calculation of Solvation Free Energies of Charged Solutes Using Mixed Cluster/Continuum Models. *J. Phys. Chem. B* **2008**, *112*, 9709−9719.
(69) Wang, X.-X.; Fu, H.; Du, D.-M.; Zhou, Z.-Y.; Zhang, A.-G.; Su, C.-F.; Ma, K.-S. The comparison of pKa determination between carbonic acid and formic acid and its application to prediction of the hydration numbers. *Chem. Phys. Lett.* **2008**, *460*, 339−342.
(70) da Silva, E. F.; Svendsen, H. F.; Merz, K. M. Explicitly Representing the Solvation Shell in Continuum Solvent Calculations. *J. Phys. Chem. A* **2009**, *113*, 6404−6409.
(71) Ding, F.; Smith, J. M.; Wang, H. First-Principles Calculation of pKa Values for Organic Acids in Nonaqueous Solution. *J. Org. Chem.* **2009**, *74*, 2679−2691.
(72) Zhang, S. A reliable and efficient first principles-based method for predicting pKa values. III. Adding explicit water molecules: Can the theoretical slope be reproduced and pKa values predicted more accurately? *J. Comput. Chem.* **2012**, *33*, 517−526.
(73) Gupta, M.; da Silva, E. F.; Svendsen, H. F. Explicit Solvation Shell Model and Continuum Solvation Models for Solvation Energy and pKa Determination of Amino Acids. *J. Chem. Theory Comput.* **2013**, *9*, 5021−5037.
(74) Marenich, A. V.; Ding, W.; Cramer, C. J.; Truhlar, D. G. Resolution of a Challenge for Solvation Modeling: Calculation of Dicarboxylic Acid Dissociation Constants Using Mixed Discrete−Continuum Solvation Models. *J. Phys. Chem. Lett.* **2012**, *3*, 1437−1442.
(75) Holler, T. P.; Hopkins, P. B. Ovothiols as Biological Antioxidants - The Thiol-Groups of Ovothiol and Glutathione are Chemically Distinct. *J. Am. Chem. Soc.* **1988**, *110*, 4837−4838.
(76) Sakurai, H.; Takeshima, S. Acid Dissociation of 2-Mercaptohistamine and Its Related Compounds. *Talanta* **1977**, *24*, 531−532.
(77) Osik, N. A.; Zelentsova, E. A.; Tsentalovich, Y. P. Kinetic Studies of Antioxidant Properties of Ovothiol A. *Antioxidants* **2021**, *10*, 1470.
(78) Jenny, K. A.; Mose, G.; Haupt, D. J.; Hondal, R. J. Oxidized Forms of Ergothioneine Are Substrates for Mammalian Thioredoxin Reductase. *Antioxidants* **2022**, *11*, 185.

https://doi.org/10.1021/acsomega.2c02506
ACS Omega 2022, 7, 31813−31821